2021

Effect of Ultra-High Pulse Frequency on the Resolution in the Electrochemical Deposition of Nickel

Abishek Balsamy Kamaraj

Natalie Reed

Murali Sundaram

Available online at www.sciencedirect.com

ScienceDirect

Procedia Manufacturing 53 (2021) 59–63

Procedia MANUFACTURING

www.elsevier.com/locate/procedia

49th SME North American Manufacturing Research Conference, NAMRC 49, Ohio, USA

Effect of Ultra-High Pulse Frequency on the resolution in the Electrochemical Deposition of Nickel

Abishek Kamaraj [a], Natalie Reed [b], Murali Sundaram [b] *

[a]*Department of Industrial and Manufacturing Engineering, Kettering University, 1700 University Ave., Flint, MI-48504, USA*

[b]*Department of Mechanical and Materials Engineering, University of Cincinnati, 2600 Clifton Ave., Cincinnati, OH-45219, USA*

* Corresponding author. Tel.: Tel.: +1-513-556-2791; fax: +1-513-556-3390. *E-mail address:* murali.sundaram@uc.edu

Abstract

Using localized electrochemical deposition (LECD) as a mask-less direct writing methodology, metal shapes are printed. The electrochemical double-layer capacitance at ultra-high frequencies is hypothesized to cause a localized deposition and the effect of pulse frequency on the current density is modeled to predict the deposition resolution and rate of deposition. Experimental results confirm that the deposition resolution and efficiency of the LECD process increase with the increase of pulse frequency. Deposition resolution 80% smaller than the tool diameter is feasible in the LECD of nickel used with a ø 250 µm tool at 1 MHz pulsed power.

Keywords: Electroforming; Modeling; Resolution

1. Introduction

Electrochemical deposition (ECD) is an essential enabling technology for precision manufacturing processes. ECD reduces metal cations from an electrolyte bath onto a substrate (cathode) to form metal deposits. This deposition can be in the form of a surface coating (electroplating) [1, 2], electroforming [3, 4], or localized electrodeposition [5-7]. The localization of the electrochemical deposition can be achieved by using a micro-tool electrode [5] or by confining the electrolyte using a jet [6], mask [8], or a meniscus [9]. The possibility of combining electrodeposition with CNC control to achieve solid freeform fabrication was discussed and fractal deposits were reported in [3, 10]. Combining the layer by layer manufacturing principles of additive manufacturing (AM) with localized electrochemical deposition (LECD) has enabled the mask-less electrochemical additive manufacturing (ECAM) process [11]. The resolution of a manufacturing process can be described as its capability of making the smallest distinguishable feature. For example, the minimum line width represents the resolution of a laser-based process [12]. The resolution of LECD (i.e. the smallest size of the deposit) is influenced by several process parameters [3, 5, 13-15] and particularly limited by the diameter (or cross-section size) of the anode used in the process. By understanding the effects of pulse frequency on the resolution in the electrochemical deposition, this work has demonstrated the feasibility of achieving deposit sizes significantly smaller than the diameter of the tool electrode and thus improves the resolution of the ECAM process.

Pulsed power has been shown to produce nanocrystalline electrodeposits with superior material properties [4]. A study on electrodeposited films of a Ni-Co alloy discovered that smoother morphology occurs in deposits made with higher frequencies and lower current densities [16]. Two other studies on electrodeposited coatings made using different composites similarly found that higher pulse frequencies result in smoother surface morphology [17, 18]. A study on Co-W alloy electroplating found that the smoothness of the deposits and the efficiency of the deposition were improved at higher pulse frequency [19]. Using an ultra-high frequency pulsed power has increased the resolution in the electrochemical machining (ECM) process due to the effects of electrochemical double-

10.1016/j.promfg.2021.06.010

layer capacitance [20]. The dynamic effect of pulse frequency on the machined hole diameter was demonstrated by varying the frequency during electrochemical machining [21]. A simulation of the machining using the time constant calculated based on the electrochemical double-layer capacitance showed that the machining gap decreased with shorter machining time [22]. In another study that used a custom made electrostatic induction feeding system, nanosecond pulses were applied to achieve precise micro-holes in stainless steel [23]. However, the machining time was found to increase with increasing the pulse frequency during ECM [24]. The double-layer capacitance and pulse power have also been used in electrolyte jet machining to improve the precision of the process [25]. Based on these previous studies, the electrochemical double-layer capacitance at ultra-high frequencies is hypothesized in this work to cause a localized deposition and the effect of pulse frequency is mathematically modeled using an equivalent electrical circuit to predict the deposit resolution.

2. Modeling the effect of pulse frequency on the current density

During LECD, the positively charged tool (anode) attracts negative ions which form a layer at the anode surface. This layer of negative ions attracts positive ions which form a layer of positive ions around the tool. These layers of opposing charge essentially act as two capacitors – one each at the interface of the electrolyte with the tool and the substrate respectively [20]. The double-layer capacitance is considered to be the reason for the confinement of the deposition under high-frequency pulse conditions. An equivalent electrical circuit is given in Figure 1, which shows the representation of double-layer capacitance (C_{dl}) and electrolyte resistance (R). The double-layer makes the electrochemical cell effectively an RC circuit with a time constant (τ=R C_{dl}). Thus, at larger distances, the deposition current will be limited under certain pulse conditions.

The period of the pulse wave sets the time limit for the current to get from the tool to the cathode. This means that at a certain distance X on the cathode away from the tool, the resistance caused by the electrolyte is large enough to prevent the double-layer from being fully charged. Therefore, beyond this point, the material cannot be deposited. Since pulse frequency is inversely related to the period of the pulse wave, this also explains why the diameter of the deposit might become smaller at higher frequencies.

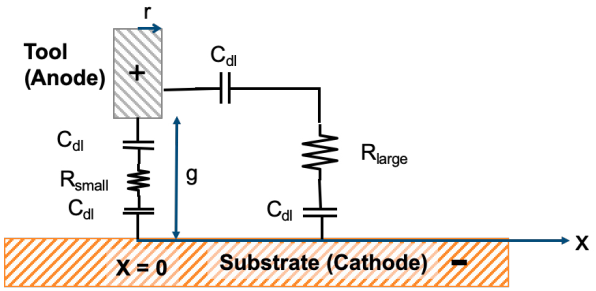

Fig. 1. Equivalent circuit of the tool-substrate interface.

At higher pulse frequencies, there is not enough time for the current to reach farther positions on the cathode and achieve a deposit. An equation for current in the model circuit can be defined using Kirchhoff's law as shown in Eq. (1).

$$\frac{dV}{dt} = R\frac{dI}{dt} + \frac{2}{c_{dl}}I \tag{1}$$

where V is the voltage supplied, R is the resistance of the electrolyte, c_{dl} is the capacitance of the double layer, dt is the time and I is the current. Solving Eq 1 for current and applying ohm's law, results in Eq. (2).

$$I = \frac{V}{Z_{eq}} e^{\frac{-2t}{Rc_{dl}}} \tag{2}$$

where Z_{eq} is the equivalent impedance in the circuit. The equivalent impedance of the circuit Z_{eq} is defined in Eq. (3).

$$Z_{eq} = R + \frac{2}{j\omega c_{dl}} \tag{3}$$

where j is the imaginary unit, ω is the angular frequency of the voltage supplied.

By changing variables to be area independent, Eq. (2) can be used to determine the current density (i) in the circuit as given in Eq. (4). Capacitance is substituted with a capacitance per unit area (c_a) and resistance is accounted for by resistivity (ρ) and the distance in the electrolyte (d).

$$\mathrm{i} = \frac{V}{\left[\rho d + \frac{2}{j\omega c_a}\right]} e^{\frac{-2t}{\rho d c_a}} \tag{4}$$

Eq. (4) shows that for a given voltage the current density on any point on the cathode is a function of the distance of that point from the tool electrode. The shortest distance traveled by the current in the electrolyte (d) is calculated using Eq. (5).

$$d = \begin{cases} g & if\ x \le r \\ \sqrt{(x-r)^2 + g^2} & if\ x > r \end{cases} \tag{5}$$

where x is the horizontal distance from the axis on the cathode, r is the radius of the tool, and g is the interelectrode gap as shown in Figure 1.

The values of the model parameters are listed in Table 1. The normalized current density values at each location across the cathode for the four different frequencies were determined from the current response calculated using Eq. (2) and the distribution of normalized peak current densities is shown in Figure 2.

Table 1. Process parameters used in the mathematical model.

Parameters	Values
Applied voltage V (V)	5 V (Peak to peak)
Electrolyte resistivity ρ ($\Omega \cdot$ cm)	500
Double-layer capacitance c_{dl} (μF/cm^2)	50
Tool radius r (μm)	125
Inter-electrode gap g (μm)	10
Modeled plate dimension x (mm)	0 – 3
Duty cycle	75%
Pulse frequency (kHz)	2, 10, 100, 1000

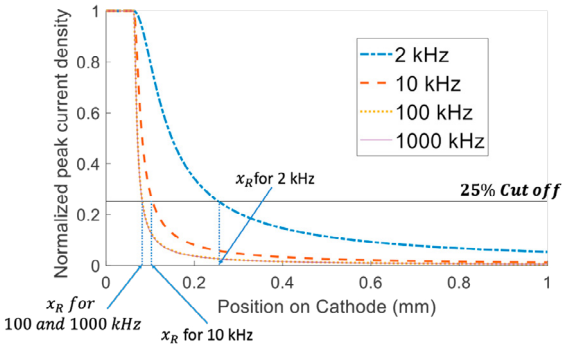

Fig. 2. Normalized peak current density distributions for multiple frequencies along the length of the cathode.

The current density for the lower frequency deposition shows a wider distribution implying a lower resolution of the deposition. Model results at higher frequencies indicate better confinement of the current density leading to a higher resolution of the deposit.

Based on the experimental observations, 25% of the peak current density for a given frequency was used to define the radius of the deposit (x_R) expected at that frequency. The deposition resolution (D_R) was determined for each of the four frequencies used in the experimentation as given in Eq. (6).

$$D_R = 2 \times x_R \quad (6)$$

3. Experimentation

The experimental setup used in this study and examples of 3D shapes made by LECD is shown in Figure 3. Localized electrochemical deposition of nickel pillars was made using a precision 3-axis stage with a stepper motor resolution of 1.5 µm, by supplying a 5V square waved pulse current with 75% duty cycle at four different frequencies (2 kHz, 10 kHz, 100 kHz, 1000 kHz) between a brass cathode and a side insulated Ø 250 µm platinum anode in an electrochemical cell made of Watts Nickel Bath (240 g $NiSO_4$, 45 g $NiCl_2$, 30 g H_3BO_3 per liter of distilled water). Images of the deposited pillars were obtained using a scanning electron microscope (SEM) as shown in Figure 4.

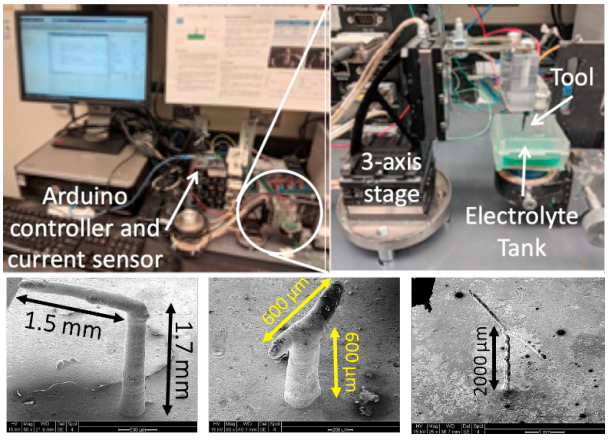

Fig. 3. Experimental setup and examples of 3D shapes made.

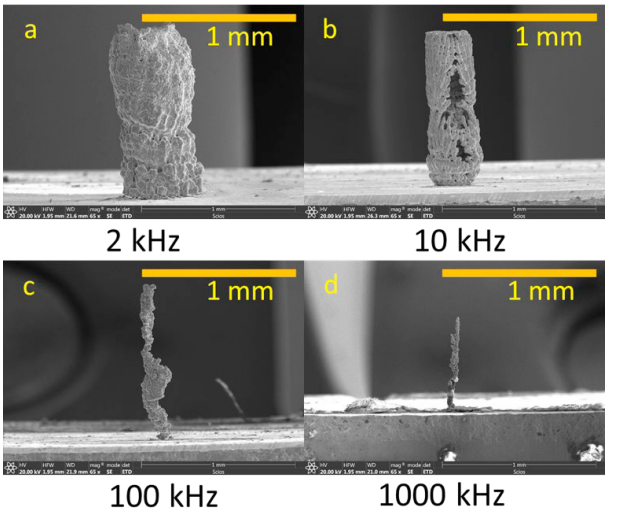

Fig. 4. SEM images of electrodeposited pillars under varying pulse frequencies.

The deposition resolutions predicted by the model were compared with the experimental results (average of 6 values) as seen in Figure 5.

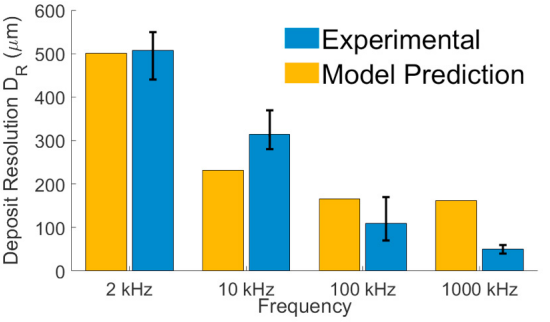

Fig. 5. SEM images of electrodeposited pillars under varying pulse frequencies.

The model predicts the deposit diameters within 20% of the experimental values for the frequencies from 2 – 100 kHz. It over predicts the deposit size at 1000 kHz. This might be because the model does not take into effect the ion depletion and the charge concentration effects which might cause a further reduction in deposit size. However, the overall trend of the model predictions is in agreement with the proposed hypothesis that the double layer capacitance causes the smaller size of deposits in ECAM under ultra-high frequencies leading to improved deposition resolution.

4. Process efficiency of LECD and the accuracy of prediction of the rate of deposition under varying pulse frequencies

Figure 6 shows seven layers of vertical deposition of a nickel pillar under various frequencies.

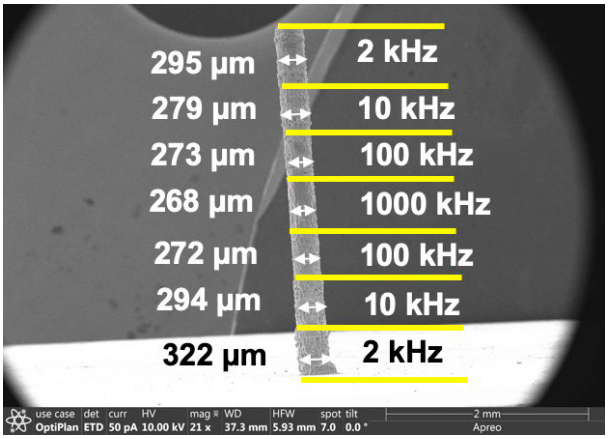

Fig. 6. SEM image of a nickel pillar manufactured at varying pulse frequency conditions.

The deposition frequency started with 2 kHz (Layer 1 at the bottom) and increased in steps to 1000 kHz (Layer 4 in the middle) during the vertical growth of the pillar and subsequently, the frequency was reduced back to 2 kHz (Layer 7 at the top) in steps. The deposit diameters showed the same trend of reduction in diameter at higher frequencies. Diameter measurements taken from the SEM image in Figure 6 show a significant narrowing of the pillar in the middle layers where higher pulse frequencies were used. From the experimental results, we do see a difference in the deposition sizes when the pillars are made individually vs varying frequency within a single pillar. This is clear from the diameter comparison between Fig 4. (separate pillars) and Fig. 6 (Same pillar). A couple of probable causes for this phenomenon are the current density concentration on the newly formed pillar and the affinity for nickel to be deposited on nickel compared to the substrate. Earlier electrochemical studies have established the effect of current density concentrating on the sharp corners and edges. This higher current density on the printed larger pillar could have diminished the effect of diameter reduction seen from the pulse frequency change.

Figure 7 shows a graph of the vertical growth of the pillar overtime during this deposition. It can be seen from this graph that lower and higher pulse frequencies result in a slower and faster rate of vertical depositions respectively. The average current density is also shown for each layer of deposition in Figure 7. These current densities are about 17 A/cm^2 with some minor variations. According to Faraday's law of electrolysis, the mass of the deposition is proportional to the product of current and time. Assuming a constant density of the deposit, this means that if the vertical deposition rate changes, the diameter of the deposit must change inversely so that a consistent rate of overall deposition is maintained. This is seen in Figure 6 from the reduction of diameter (i.e. higher resolution) with higher frequency. Moreover, the nonlinearity noticed in this change of resolution with frequencies reveals that the change of frequency also affects the efficiency of the deposition process.

The theoretical rate of deposit (R_T) is given by Eq. (7).

$$R_T = \frac{IM}{Fz\rho} \quad (7)$$

where I is current, F is Faraday's constant, M, z, and ρ are the molar mass, valency number, and density of nickel respectively.

The values of the rate of deposition shown in Table 2 reveal a positive correlation of deposition efficiency of the LECD process with the pulse frequency used. For example, the rate of deposition doubles from 15 m^3/s to 32 m^3/s when the pulse frequency is increased from 10 kHz to 1000 kHz. The theoretical prediction of the rate of deposition does not vary as widely as the experimental rate as seen in Table 2. This might be due to the theoretical value assuming that the deposit is fully dense with 0% porosity. At high frequencies, the cations that are depleted during the on-time, due to the reduction reaction, do not get replenished sufficiently in the limited off-time [13]. This leads to a more porous deposit [7]. This could explain the discrepancy between theoretical and experimental deposition rates.

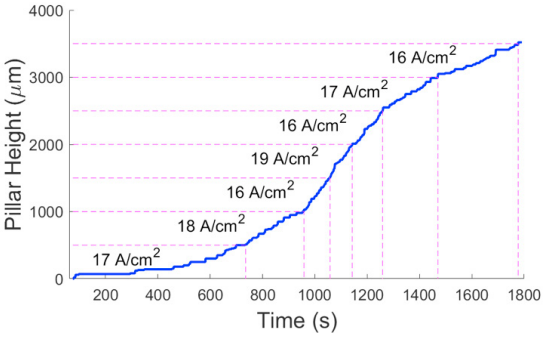

Fig. 7. Graph of vertical deposit over time with varying pulse frequency.

Table 2. The efficiency of the LECD process at different pulse frequencies.

Layer	Pulse frequency f (kHz)	Experimental rate of deposition R_E (m^3/s x 10^{-14}),	Theoretical rate of deposition R_T (m^3/s x 10^{-14}),	% error in theoretical prediction $\left\|\frac{R_T-R_E}{R_T}\right\| X100$
1	2	6.3	28.8	78
2	10	15.0	29.8	50
3	100	28.2	26.2	8
4	1000	32.0	31.6	1
5	100	25.2	26.6	5
6	10	14.6	27.8	47
7	2	11.4	27.3	58

5. Conclusions

A mathematical model of current density distribution over the cathode during the LECD process was developed and used to predict the resolution of depositions performed using different frequencies of pulse power. The overall trend of the predicted deposition resolution agrees with the proposed hypothesis that the double layer capacitance causes the smaller size of deposits under ultra-high frequencies of pulse power, leading to improved deposition resolution. Deposit resolution

40 to 80% smaller than the tool diameter is obtained when the frequency of the pulse power supplied is increased to 100 kHz and 1000 kHz. The effect of ultra-high pulse frequency on the resolution in the electrochemical deposition of nickel is demonstrated by changing the pulse frequency within a single deposit which resulted in a deposition with varying deposit resolutions. Deposition efficiency (i.e. rate of deposition) increases with the increase in pulse frequencies and the percentage error of theoretical prediction of the rate of deposition is within 1-8 % for experimental values of deposition rates at 100 kHz and 1000 kHz pulse frequencies.

Acknowledgments

Financial support provided by the National Science Foundation under Grant Nos. CMMI- 1955842 and CMMI-1454181 are acknowledged.

References

[1] Masuku ES, Mileham AR, Hardisty H, Bramley AN, Johal C, Detassis P. A Finite Element Simulation of the Electroplating Process. CIRP Annals. 2002;51:169-72.
[2] Islam A, Hansen HN, Tang PT. Direct electroplating of plastic for advanced electrical applications. CIRP Annals. 2017;66:209-12.
[3] McGeough JA, Leu MC, Rajurkar KP, De Silva AKM, Liu Q. Electroforming Process and Application to Micro/Macro Manufacturing. CIRP Annals. 2001;50:499-514.
[4] Zhu D, Lei WN, Qu NS, Xu HY. Nanocrystaline Electroforming Process. CIRP Annals. 2002;51:173-6.
[5] Madden JD, Hunter IW. Three-dimensional microfabrication by localized electrochemical deposition. Journal of Microelectromechanical Systems. 1996;5:24-32.
[6] Kunieda M, Katoh R, Mori Y. Rapid Prototyping by Selective Electrodeposition Using Electrolyte Jet. CIRP Annals. 1998;47:161-4.
[7] Kamaraj A, Lewis S, Sundaram M. Numerical study of localized electrochemical deposition for micro electrochemical additive manufacturing. Procedia CIRP. 2016;42:788-92.
[8] Zhu D, Zeng YB. Micro electroforming of high-aspect-ratio metallic microstructures by using a movable mask. CIRP Annals. 2008;57:227-30.
[9] Hu J, Yu M-F. Meniscus-Confined Three-Dimensional Electrodeposition for Direct Writing of Wire Bonds. Science. 2010;329:313.
[10] He Z, Zhou JG, Tseng AA. Feasibility study of chemical liquid deposition based solid freeform fabrication. Materials & Design. 2000;21:83-92.
[11] Sundaram MM, Kamaraj AB, Kumar VS. Mask-Less Electrochemical Additive Manufacturing: A Feasibility Study. Journal of Manufacturing Science and Engineering. 2015;137:021006-.
[12] Overmeyer L, Hohnholz A, Suttmann O, Kaierle S. Multi-material laser direct writing of aerosol jet layered polymers. CIRP Annals. 2019;68:217-20.
[13] Kamaraj AB, Sundaram M. A study on the effect of inter-electrode gap and pulse voltage on current density in electrochemical additive manufacturing. Journal of Applied Electrochemistry. 2018;48:463-9.
[14] Lin JC, Chang TK, Yang JH, Chen YS, Chuang CL. Localized electrochemical deposition of micrometer copper columns by pulse plating. Electrochimica Acta. 2010;55:1888-94.
[15] Wang C-Y, Lin J-C, Chang Y-C, Tseng Y-T, Ciou Y-J, Hwang Y-R. Fabrication of Cu-Zn Alloy Micropillars by Potentiostatic Localized Electrochemical Deposition. Journal of The Electrochemical Society. 2019;166:E252-E62.
[16] Chung CK, Chang WT. Effect of pulse frequency and current density on anomalous composition and nanomechanical property of electrodeposited Ni–Co films. Thin Solid Films. 2009;517:4800-4.
[17] Jiang S, Guo Z, Deng Y, Dong H, Li X, Liu J. Effect of pulse frequency on the one-step preparation of superhydrophobic surface by pulse electrodeposition. Applied Surface Science. 2018;458:603-11.
[18] Yang Y, Cheng YF. Fabrication of Ni–Co–SiC composite coatings by pulse electrodeposition — Effects of duty cycle and pulse frequency. Surface and Coatings Technology. 2013;216:282-8.
[19] Donten M, Stojek Z. Pulse electroplating of rich-in-tungsten thin layers of amorphous Co-W alloys. Journal of Applied Electrochemistry. 1996;26:665-72.
[20] Schuster R, Kirchner V, Allongue P, Ertl G. Electrochemical Micromachining. Science. 2000;289:98-101.
[21] Jo CH, Kim BH, Chu CN. Micro electrochemical machining for complex internal micro features. CIRP Annals - Manufacturing Technology. 2009;58:181-4.
[22] Kim BH, Na CW, Lee YS, Choi DK, Chu CN. Micro Electrochemical Machining of 3D Micro Structure Using Dilute Sulfuric Acid. CIRP Annals - Manufacturing Technology. 2005;54:191-4.
[23] Koyano T, Kunieda M. Micro electrochemical machining using electrostatic induction feeding method. CIRP Annals. 2013;62:175-8.
[24] Mithu MAH, Fantoni G, Ciampi J, Santochi M. On how tool geometry, applied frequency and machining parameters influence electrochemical microdrilling. CIRP Journal of Manufacturing Science and Technology. 2012;5:202-13.
[25] Kawanaka T, Kunieda M. Mirror-like finishing by electrolyte jet machining. CIRP Annals. 2015;64:237-40.